JOURNAL OF GEOPHYSICAL RESEARCH, VOL. 104, NO. D1, PAGES 1699–1704, JANUARY 20, 1999

An improved fast-response vacuum-UV resonance fluorescence CO instrument

Christoph Gerbig, Sandra Schmitgen, Dieter Kley, and Andreas Volz-Thomas
Institut für Chemie und Dynamik der Geosphäre, Forschungszentrum Jülich, Jülich, Germany

Ken Dewey
Meteorological Research Flight, Atmospheric Chemistry Group, U.K. Meteorological Office, Bracknell, England
Defense Research Agency, Farnborough, England

Dieter Haaks
AERO-LASER GmbH, Garmisch-Partenkirchen, Germany

Abstract. The fast-response resonance fluorescence instrument for the airborne measurement of carbon monoxide described by *Gerbig et al.* [1996] was modified by implementing an improved optical filter with more efficient optics and an optimized resonance lamp. Besides reductions in size and weight, the new instrument achieves a sensitivity 10 times higher, a lower background (65 ppb compared with 250 ppb), and a faster time response (<0.1s) than the original instrument. The precision is ±1.5 ppb at an atmospheric mixing ratio of 100 ppb CO, and the detection limit is 3 ppb (2σ) for an integration time of 1 s. First results from the North Atlantic Regional Aerosol Characterization Experiment (ACE-2) campaign during July 1997, when the new instrument was deployed aboard the U.K. Meteorological Office C-130 aircraft, are used to demonstrate the performance of the new instrument.

1. Introduction

Carbon monoxide has a strong influence on global tropospheric chemistry [*Fishman and Crutzen*, 1978]. Anthropogenic emissions constitute a major source of CO in the troposphere [*Seiler*, 1974; *Logan et al.*, 1981]. Further sources are the oxidation of methane and hydrocarbons, as well as biomass burning [*Crutzen and Andreae*, 1990]. Because of its photochemical lifetime of about 1 month in summer and its insolubility, CO is an excellent tracer for investigating the transport of polluted air masses into cleaner regions [*Fishman and Seiler*, 1983; *Parrish et al.*, 1993]. Because of the stratospheric sink of CO it can also be used to identify air masses of stratospheric origin [*Hipskind et al.*, 1987]. A large fraction of the transport of polluted air masses may occur above the planetary boundary layer (PBL), originating from exchange processes such as convection between the polluted PBL and the free troposphere [*Pickering et al.*, 1992]. Thus aircraft measurements are needed in order to obtain a better experimental database for estimating the total amount of ozone and precursors that are transported from continental sources into remote regions.

Techniques that have been used for in situ measurement of CO aboard aircraft are (besides gas chromatography [see *Marenco*, 1989], which provides only a discontinuous record) the HgO method [*Seiler et al.*, 1980], infrared absorption by gas filter correlation (GFC) or nondispersive infrared spectroscopy (NDIR) [*Dickerson and Delany*, 1987]), tunable diode laser absorption spectroscopy (TDLAS) [*Sachse et al.*, 1987; *Roths et al.*, 1996] and resonance fluorescence in the fourth positive band of CO (hereinafter denoted VURF) [*Volz and Kley*, 1985; *Gerbig et al.*, 1996]. Only TDLAS and VURF exhibit sufficient sensitivity and time response for precisely measuring ambient CO mixing ratios at a time resolution of the order of 1 s, as is required aboard aircrafts.

The VURF instrument that was originally built for balloonborne measurements of stratospheric CO [*Volz and Kley*, 1985] was flown successfully aboard the Hercules C-130 after several modifications [*Gerbig et al.*, 1996]. These authors concluded on the basis of laboratory experiments and theoretical considerations that a large fraction of the observed background signal, which determines the achievable precision and detection limit, was not due to stray light, e.g. from the walls of the fluorescence chamber, but originated from continuum resonance Raman scattering by oxygen molecules. This finding put a new light on the required reduction of stray light as originally proposed by *Volz and Kley* [1985] and opened the door for a redesign of the instrument in order to improve its performance. A further reason for the redesign was to make the technique available to a wider scientific community, which was realized in the framework of a technology transfer contract. In this paper the new instrument is described, and a few examples of measurements over the Atlantic during ACE2 are shown to illustrate its performance.

2. The New Instrument

The new instrument is shown schematically in Figure 1. It consists of the same principal components as the old instrument, namely, a resonance lamp excited by a RF discharge, an optical filter for selection of the appropriate wavelength interval around 150 nm, which images the lamp into the RF chamber, where the fluorescence is viewed at a right angle by means of a photomultiplier tube (PMT) with suprasil optics. The

Paper number 1998JD100031.
0148-0227/99/1998JD100031$09.00

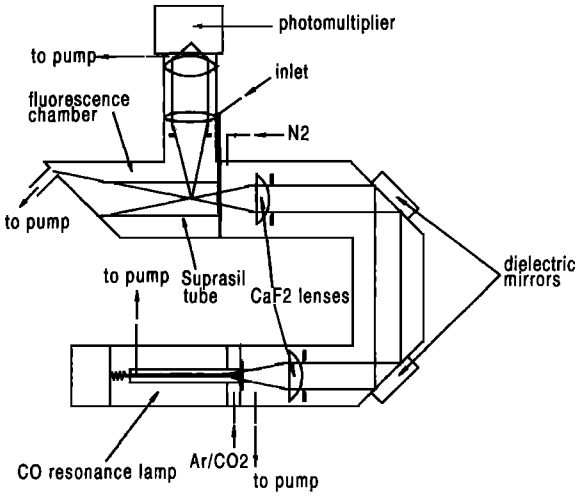

Figure 1. Schematic of the new instrument.

optical filter is completely revised. Instead of using the imaging properties of the grating, the discharge volume of the CO resonance lamp is imaged into the fluorescence chamber by means of two CaF_2 lenses. The two dielectric mirrors, which provide the spectral band path (bandwidth of 8 nm full width at half maximum (FWHM) at approximately 150 nm; see Figure 2), are placed in the parallel part of the light beam. Because of the larger aperture ($f/1.8$ instead of $f/4.5$ in the original instrument) and the better geometry of the imaging system (i.e., round apertures instead of slits) the new design, in addition to being smaller and lighter, provides a much higher sensitivity and a better signal-to-noise ratio. Because its volume is 10 times smaller, the new optical filter requires a much smaller N_2 flow than the old monochromator for flushing. Flushing is necessary to avoid absorption of the radiation by the Schumann-Runge continuum of molecular oxygen or by impurities, in particular CO. The optical filter is made from brass that is coated black by a layer of CuO instead of using organic dyes for blackening.

The better imaging properties of the new optical filter allow for additional improvements concerning the dimensions of the light source and the PMT. Instead of the original front end PMT (0.5 inch or 1.27 cm diameter) a small side-on PMT is used (quantum efficiency 35% at 180 nm, dark count rate 20 cps), and a capillary discharge is used for the light source, providing a higher flux density and similar dimensions to the photocathode of the PMT.

The discharge volume of the lamp is imaged (1:1) into the fluorescence chamber by the $f/1.8$ optics of the optical filter. To make use of the better geometry of the focus within the fluorescence chamber, the imaging optics for the fluorescent radiation are changed from a single suprasil lens (1:1 image) to a combination of two suprasil lenses (2:1 reduction).

The combination of the above described changes increased the sensitivity of the instrument by a factor of 12 ($f = 5$ from the larger aperture of the optical filter, $f = 2$ from the improved PMT optics and the higher quantum efficiency, and the rest from the higher flux density of the lamp and reduced self-absorption in the discharge). The background signal increased only by about a factor of 3, leading to an increase in the signal-to-noise ratio by a factor of 5 (assuming a sample gas mixing ratio of 100 ppb CO). When expressed in CO equivalents (i.e., divided by the sensitivity), the background signal decreased to a value of 65 ppb, compared with 250 ppb for the version of the instrument described by *Gerbig et al.* [1996]. Reasons for the decrease of the background expressed in CO equivalents are the better discrimination of radiation in the wavelength region above 160 nm due to the narrower bandwidth of the filter (see Figure 2), and the better geometry of the imaging system leading to reduced stray light.

Further modifications were made to the fluorescence chamber in order to enhance the time resolution of the instrument. The dimensions of the original fluorescence chamber were changed to minimize stray light. With the limited pumping capacity provided by the four-stage membrane pump (Vacuubrand, MZ-4) installed aboard the C-130, this resulted in a relatively long exchange time of the sampled air in the illuminated volume, which limited the time resolution of the instrument to approximately 2 s, in accordance with the maximum possible time resolution given by photon statistics. With the improved sensitivity of the new instrument it was found advantageous to improve the gas kinetic time resolution of the instrument without having to install a larger pump in the aircraft. Although the sample gas is exchanged faster in the smaller and better defined fluorescing volume, the large dead volumes of the fluorescence chamber still disturb the time resolution. In order to further enhance the exchange rate of the sample gas within the fluorescing volume, a high-quality quartz tube was installed in the fluorescence cell (see Figure 1), coaxial with the optical axis of the exciting radiation. The increase in the background signal observed upon insertion of the quartz tube was only 10%.

A homogeneous flow through the quartz tube, without reducing the time response by dead volumes, is achieved by feeding the sample gas into the tube via eight small orifices around the window between optical filter and fluorescence chamber. The air is vented into the fluorescence chamber,

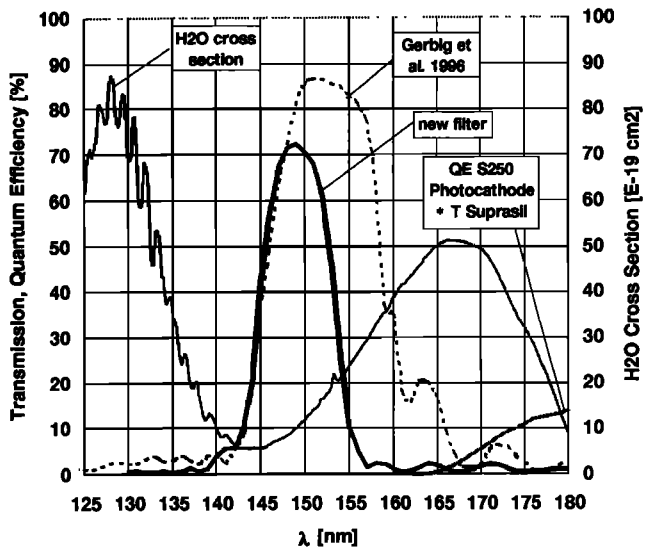

Figure 2. Transmission of the optical filter as used in the previous instrument (dashed line) and in the new design (thick solid line) together with the absorption cross section of H_2O (thin line) [*Yoshino et al.*, 1996] and the quantum efficiency of the S250 cathode used for the fluorescence detection multiplied with the transmission of the suprasil optics (gray line).

which is connected to the pump at the end of the light trap and at the PMT flange, in order to provide a well-defined air flow.

With the conservative assumption of a laminar flow profile in the quartz tube (the Reynolds number is about 1300), the residence time of the sample gas in the fluorescing volume which is imaged onto the cathode of the PMT (length $\approx$ 1 cm) is calculated to be approximately 10 ms, at a pressure of 7.5 mbar and a volume flow rate of 1.4 L min^{-1} as provided by the four-stage membrane pump used aboard the C-130. Experimentally, the time constant was determined to be <0.1 s, as limited by the 10 Hz sampling rate of the data acquisition system.

When using only the dielectric mirrors for wave length selection in the optical filter (grating used in zeroth order), *Gerbig et al.* [1996] observed a small positive interference by atmospheric water vapor, which overruled the expected negative interference due to absorption of the fluorescence radiation by water vapor. The positive interference was identified as being caused by photodissociation of H_2O at wavelengths below 135.7 nm and subsequent fluorescence of the excited OH radicals at wavelengths around 310 nm.

Figure 2 shows the absorption cross section of water vapor [*Yoshino et al.*, 1996] together with the transmission of the optical filter used in the previous instrument (grating in zeroth order) and of the new optical filter. The dielectric mirrors used in the new optical filter provide a better discrimination of radiation in the wavelength region above 160 nm, where the fluorescence is detected, than the previously used filter. The new optical filter also provides about a factor of 7 better discrimination in the wavelength range below 136 nm. Indeed, no increase in the fluorescence signal was detected in laboratory tests, where water vapor was added to zero air (up to 100% relative humidity at 20°).

3. Laboratory Tests (Operating Conditions)

The influence of pressure changes in the whole system is shown in Figure 3. Since all flows are connected to the same pump, the pressure is the same for all volumes (i.e., fluorescence chamber, optical filter, and discharge lamp). The sensitivity shows a fairly broad maximum between about 7 and 11 mbar, while the background expressed in CO equivalents has a broad minimum between 5 and 7 mbar. This results in a broad

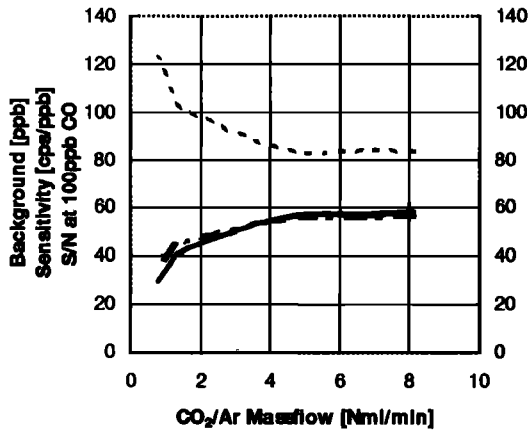

Figure 4. Sensitivity (solid line), background (dotted line) and signal-to-noise ratio for 100 ppb CO (dashed-dotted line) as function of the lamp flow rate.

maximum of the signal-to-noise ratio between 7 and 9 mbar. Most of the pressure dependence arises from the changes in the CO concentration (at constant mixing ratio) and from absorption of the exciting radiation due to O_2 in the fluorescence chamber [*Volz and Kley*, 1985].

Figure 4 shows the dependence of the sensitivity and the background signal (expressed in CO equivalents) on the CO_2/Ar flow rate through the new lamp at constant pressure (7.5 mbar). For very small flows, the sensitivity increases with increasing flow rate and reaches an almost constant value at flow rates of >5 mL (STP) min^{-1}. The background decreases with increasing flow and becomes also constant (within <5%) for flow rates >5 mL (STP) min^{-1}. The old lamp, because of its much larger volume, required flow rates of >40 mL (STP) min^{-1} in order to reach optimum performance. Obviously, the smaller diameter of the lamp significantly reduces the residence time of the gas mixture in the discharge and thus the self absorption by ground state CO molecules that arise from the decomposition of the CO_2.

Figure 5 shows the dependency of the new instrument's sensitivity and background (expressed in CO-equivalents) on the N_2 flow in the optical filter at a constant pressure of 7.5 mbar. For nitrogen flow rates of <8 mL (STP) min^{-1}, both

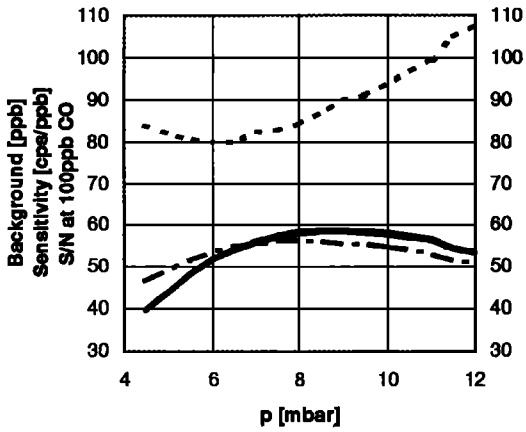

Figure 3. Sensitivity (solid line), background (dotted line), and signal-to-noise ratio for 100 ppb CO (dashed-dotted line) as function of the instrument pressure.

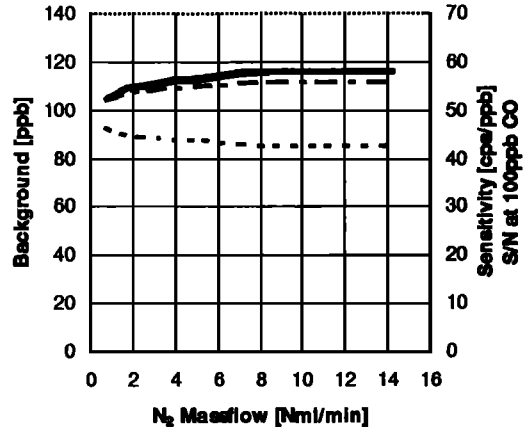

Figure 5. Sensitivity (solid line), background (dotted line) and signal-to-noise ratio for 100 ppb CO (dashed-dotted line) as function of the flow rate of N_2.

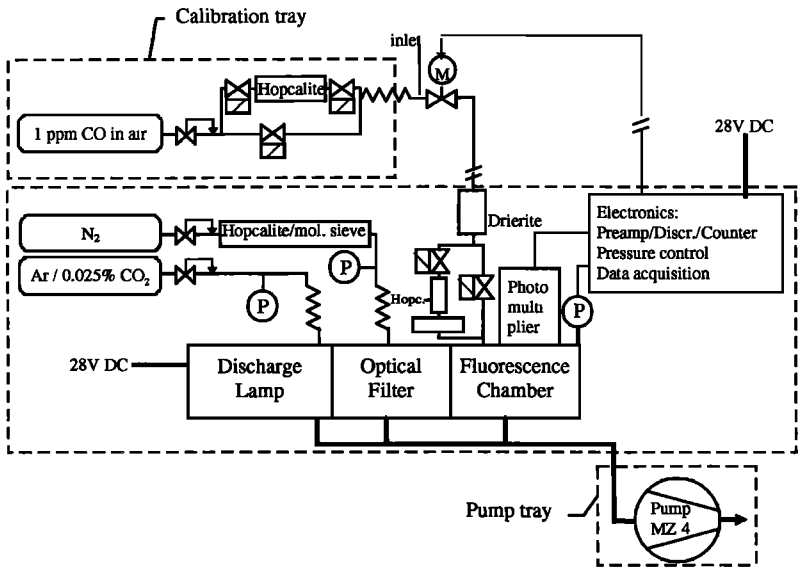

Figure 6. Flight setup of the resonance fluorescence instrument.

sensitivity and background signal remain constant at levels of 58 cps ppb^{-1} and 84 ppb (CO equivalents), respectively. A 10% reduction in sensitivity and an increase of 7 ppb in the background are observed when the flow rate is reduced to about 1 mL (STP) min^{-1}. Also shown in Figure 4 is the corresponding signal-to-noise ratio calculated for a mixing ratio of 100 ppb CO. A flow rate of 5 mL (STP) min^{-1} was chosen for the field measurements.

4. Flight Setup and Performance Assessment

The setup used for the airborne measurements aboard the C-130 is shown in Figure 6. The sample gas is taken from the starboard air sampling pipe (ASP) of the aircraft using a PFA tube with 1/8 inch OD and a length of about 15 m. This distance is determined by the only available position for the instrument aboard the aircraft. The small residual influence of water vapor due to absorption of the fluorescence radiation (a mixing ratio of 2% H_2O causes a decrease in the fluorescence signal of 10%) is removed by passing the sampled air over a bed of Drierite ($CaSO_4$ with humidity indicator) contained in a 10-cm-long, 7-mm-ID Pyrex tube. Absorption of CO by the drying agent was not observed within the experimental uncertainties of 1%, and the response time of the instrument was not measurably deteriorated.

Close to the ASP, a piezo-driven valve (Fa. Bürkert, model 6115) is installed in the inlet line. The valve is adjusted by the program used for data acquisition and controls the pressure inside the fluorescence chamber at 7.5 ± 0.1 mbar for ambient pressures between 1013 and 175 mbar, which keeps the variation of the CO signal below 0.5%. The fluorescence chamber, resonance lamp, and optical filter are connected to a four-stage membrane pump (Vacubrand, model MZ4, all heads in series). The gases for the lamp and the optical filter are contained in two gas bottles, each with a volume of two liters. The filter is continuously flushed with a flow of N_2 (5 mL (STP) min^{-1}, purity 99.999%), which is purified from traces of CO, CO_2, and H_2O by passing it over a bed of hopcalite and molecular sieve.

In situ calibration of the instrument is achieved by injecting a standard (440 ppb CO in air) into the sampling line, close to the control valve, at flow rates slightly higher than the sample flow rate. The small excess flow (about 10 mL (STP) min^{-1}) is vented into the ASP. The in-flight standard is compared with a primary standard (1 ppm CO in air; Messer Griesheim) before each flight. For determination of the background signal, the calibration standard is passed through a Hopcalite scrubber, which quantitatively removes the CO to levels <1 ppb. In addition, the background signal is determined by switching a Hopcalite scrubber into the sample flow between the inlet tube and the fluorescence chamber. This enables detection of possible errors due to leaks within the inlet tube or the water trap.

The resonance fluorescence signal depends on the pressures in the chamber and in the lamp, as well as on the flow rates of CO_2/Ar and nitrogen through the lamp and the optical filter, respectively. The stability of these parameters is, therefore, of importance for the accuracy of the measurement. The flow rates of N_2 and CO_2/Ar are held constant by (vacuum referenced) pressure regulators and thermostatted capillaries. Since all flows are connected to the same pump, the pressure in the lamp and in the optical filter are maintained constant at the same level and with the same accuracy as the pressure in the RF chamber by means of the piezo valve in the inlet line.

Changes in the temperature of the lamp and of the PMT also have an influence on the instrument's sensitivity. The photoemissive yield of the PMT's photocathode decreases with temperature due to enhanced interaction of the photo electrons with lattice photons, which leads to increased loss of energy [*Spicer and Wooten*, 1963]. Laboratory testing showed a temperature dependence of −0.9%/°C for the PMT sensitivity, which is higher than the manufacturer's specification of −0.2%/°C. The temperature of the lamp has an influence on the sensitivity due to Doppler broadening of the lines and changes in the rotational distribution of the CO emission. More importantly, however, the output power of the radio frequency circuit used for excitation of the discharge in the lamp decreases significantly with increasing temperature. Therefore the lamp and PMT module are thermostatted at a

Table 1. Comparison Between the Specifications of the Original and Improved Instrument

	Gerbig et al. [1996]	This Paper
Sensitivity	6 cps/ppb	70 cps/ppb
Background	1500 cps or 250 ppb	4500 cps or 65 ppb
Precision (@ 100 ppb and 1 s)	8.2 ppb	1.5 ppb
Accuracy	5 ppb + 2.8% @ 2s	1.3 ppb + 2.4% @ 1s
Linear response	0–100 ppm	0–100 ppm
Time response	2 s	<0.1 s

temperature of 40°C, which is easy to maintain in the aircraft environment.

5. Performance of the New Instrument

In Table 1 the specifications of the new version of the instrument flown aboard the C-130 are summarized and compared to the old instrument [*Gerbig et al.*, 1996]. The new instrument achieves a much higher precision (determined by counting statistics) due to the 12 times higher sensitivity and a 4 times lower background (in CO equivalents). The accuracy is calculated from the accuracy of the calibration standard, the background and sensitivity drift and from the achieved precision determined by counting statistics. Because of improved temperature control of the critical components, background and sensitivity are less influenced by changes in ambient conditions, which leads to a better accuracy and requires less frequent calibrations. The achievable time resolution is increased from about 2 s to 0.1 s.

Since June 1997, the new instrument was deployed aboard the U.K. Meteorological Office Hercules C-130 within several European projects, i.e., the North Atlantic Regional Aerosol Characterization Experiment (ACE-2), Testing of Atmospheric Chemistry in Anticyclones (TACIA), and the U.K. National Environmental Research Council project Atmospheric Chemistry Studies in the Oceanic Environment (ACSOE). We show data from these experiments to demonstrate the in-flight performance of the instrument and the long-term stability.

In-flight calibrations and zeros lasting roughly 90 seconds were routinely performed about every 30 minutes. The behavior of the sensitivity and the background during the whole ACE-2 campaign and during the subsequent intensive flying periods (TACIA and ACSOE) is shown in Figure 7, as a function of accumulated flight hours. A slow decrease by a factor of 2 can be seen during the first 140 flight hours, which correspond to about 200 hours of operation including ground tests and pre flight preparations. The decrease of sensitivity was caused by a degradation of the lamp window. After replacement of the window, the sensitivity was restored to the original value. In addition, the sealing rings were replaced and the lamp was cleaned. No decrease of sensitivity was observed during the following intensive flying campaign. The total range in sensitivity and background changes for the individual flights were 8% and 3.5 ppb, respectively. Since the changes occur slowly, however, the deviation of the sensitivity and background from their interpolated value between consecutive calibration cycles are only ±1.3% and 0.9 ppb, respectively.

Figure 8 shows an example of the measurements made during the second flight of the second Lagrangian experiment during ACE-2 on July 17, 1997. During this flight, the C-130 flew rectangular box patterns at different altitudes, located at 36.5°N, 13.5°W, to the west of Sagres (Portugal). From 3-day back trajectories it was indicated that the air masses which were sampled during this flight period were likely influenced by anthropogenic emissions over the Iberian peninsula. The measurements shown in Figure 8 were made during the end of the rectangular pattern at 900 m, during a short profile to 2000 m and after a descent during the beginning of the next rectangular pattern at 1600 m. Fast and correlated changes in the mixing ratios of CO and ozone occurred when the aircraft changed the altitude, indicating a strong layering of different air masses with a vertical extent of 100–300 m. From the right panel of Figure 8 it can be seen clearly that the fluorescence instrument is capable of following these rapid changes within the time resolution of 1 s as determined by rate at which data were recorded during these flights. The measurements made at constant altitude also show a correlation between CO and ozone on timescale of seconds, which corresponds to a horizontal scale of a few hundred meters. The most likely explanation is that the aircraft was flying close to the undulating boundary between different air mass layers.

Also shown in Figure 8 are running averages over 60 s, which were calculated from the original data in order to simulate an instrument that has a less rapid response, e.g., a NDIR instrument like the Thermo Instruments model 48S. It is clearly seen that these averages do not show the rapid natural variations in the CO mixing ratio. Most important, on many occasions the

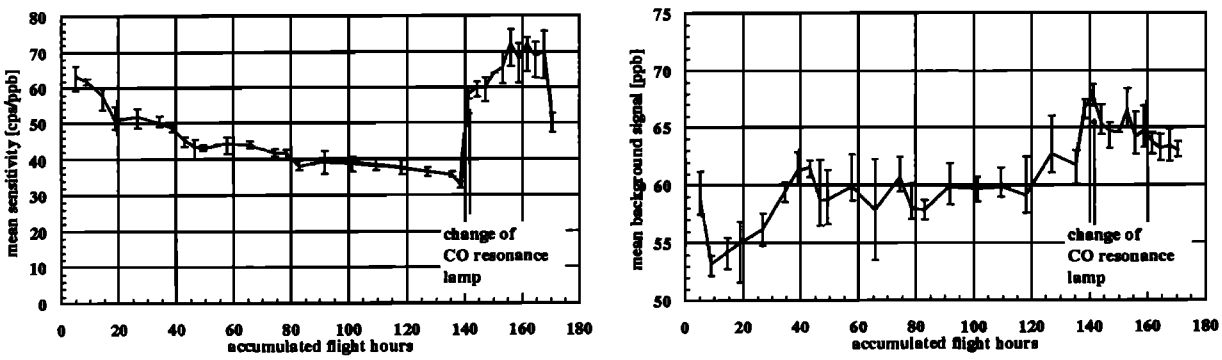

Figure 7. Average sensitivity and background signal for each flight during ACE-2 and following the TACIA and ACSOE intensive flying campaigns, plotted against the accumulated flight time. The bars indicate the maximum and minimum values for the individual flights. Note the offset of 50 ppb in the right panel.

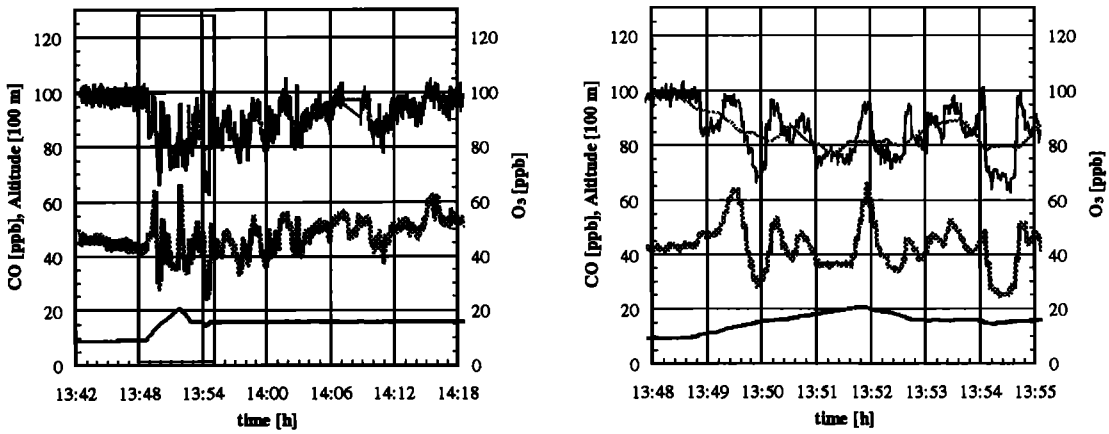

Figure 8. One-second averages of CO (top black line) and ozone mixing ratios (thick gray line) measured during flight A559 (July 17, 1997) over the North Atlantic (36.5°N, 13.5°W) and the aircraft altitude (bottom black line), with 60-s running averages of CO (thin gray line) shown to simulate a less rapid response. (right) Enlargement of the beginning of the small-spatial-scale variations due to a repeated change of air mass during the change of altitude.

distinct correlation with ozone is lost almost completely. This example clearly shows the advantage of a fast response instrument to investigate atmospheric structures on small spatial scales.

6. Conclusions

The new VURF instrument achieves a 5 times higher precision and a better time resolution (<0.1s) and is smaller in size and weight than the previous version. Data from flights during ACE-2 prove that the new instrument is able to resolve small scale natural variations in the CO mixing ratio with differences of 10 ppb within a second. The precision and time resolution of the new VURF instrument is comparable to that reached with TDLAS. Advantages of the VURF instrument, in particular for airborne measurements, are its smaller space and weight combined with less logistic demands compared to TDLAS.

Acknowledgments. The authors wish to thank the personnel and the air crew of the U.K. Meteorological Office, Meteorological Research Flight, for their assistance before and during the campaign. We also wish to thank Karsten Suhre for trajectory information. The projects ACE-2 and TACIA were funded by the Commission of the European Community, Directorate DG XI (ENV4-CT95-0032 and ENV4-CT95-0038).

References

Crutzen, J. P., and M. O. Andreae, Biomass burning in the tropics: Impact on atmospheric chemistry and biogeochemical cycles, *Science*, *250*, 1669–1678, 1990.

Dickerson, R. R., and A. C. Delany, Modification of a commercial gas filter correlation CO detector for enhanced sensitivity, *J. Atmos. Oceanic Technol.*, *5*, 424–431, 1987.

Fishman, J., and P. J. Crutzen, The origin of ozone in the troposphere, *Nature*, *274*, 855–858, 1978.

Fishman, J., and W. Seiler, Correlative nature of ozone and carbon monoxide in the troposphere: Implications for the tropospheric ozone budget, *J. Geophys. Res.*, *88*(C6), 3662–3670, 1983.

Gerbig, C., D. Kley, A. Volz-Thomas, J. Kent, K. Dewey, and D. S. McKenna, Fast-response resonance fluorescence CO measurements aboard the C-130: Instrument characterization and measurements made during NARE '93, *J. Geophys. Res.*, *101*, 29,229–29,238, 1996.

Hipskind, R. S., G. L. Gregory, G. W. Sachse, G. F. Hill, and E. F. Danielsen, Correlations between ozone and carbon monoxide in the lower stratosphere, folded tropopause, and maritime troposphere, *J. Geophys. Res.*, *92*, 2121–2130, 1987.

Logan, J. A., M. J. Prather, S. C. Wofsy, and M. B. McElroy, Tropospheric chemistry: A global perspective, *J. Geophys. Res.*, *86*(C8), 7210–7254, 1981.

Marenco, A., M. Macaigne, and S. Prieur, Meridional and vertical CO and CH_4 distributions in the background troposphere (70°N–60°S; 0–12 km altitude) from scientific aircraft measurements during the STRATOZ III experiment (June 1984), *Atmos. Environ.*, *23*, 185–200, 1989.

Parrish, D. D., J. S. Holloway, M. Trainer, P. C. Murphy, G. L. Forbes, and F. C. Fehsenfeld, Export of North American pollution to the North Atlantic Ocean, *Science*, *259*, 1436–1439, 1993.

Pickering, K. E., J. R. Scala, A. M. Thompson, W. K. Tao, and J. Simpson, Free tropospheric ozone production following entrainment of urban plumes into deep convection, *J. Geophys. Res.*, *97*, 17,985–18,000, 1992.

Roths, J., T. Zenker, U. Parchatka, F. G. Wienhold, and G. W. Harris, FLAIR, a four laser airborne infrared spectrometer for atmospheric trace-gas measurements, *Appl. Opt.*, *35*, 7075–7084, 1996.

Sachse, G. W., G. F. Hill, L. O. Wade, and M. G. Perry, Fast-response, high-precision carbon monoxide sensor using a tunable diode laser absorption technique, *J. Geophys. Res.*, *92*, 2071–2081, 1987.

Seiler, W., The cycle of atmospheric CO, *Tellus*, *24*, 116–135, 1974.

Seiler, W., H. Giehl, and P. Roggendorf, Detection of carbon monoxide and hydrogen by conversion of mercury oxide to mercury vapor, *Atmos. Technol.*, *12*, 40–47, 1980.

Spicer, W. E., and F. Wooten, Photoemission and photomultipliers, *Proc. IEEE*, *51*, 1119–1126, 1963.

Volz, A., and D. Kley, A resonance fluorescence instrument for the in-situ measurement of atmospheric carbon monoxide, *J. Atmos. Chem.*, *2*, 345–357, 1985.

Yoshino, K., J. R. Esmond, W. H. Parkinson, K. Ito, and T. Matsui, Absorption cross section measurements of water vapor in the wavelength region 120 to 180 nm, *Chem. Phys.*, *211*, 387–391, 1996.

K. Dewey, Defense Research Agency, Farnborough, Hampshire GU1 46TD, England, United Kingdom.

C. Gerbig, D. Kley, S. Schmitgen, and A. Volz-Thomas, ICG-2, Forschungszentrum Jülich, Postfach 1913, D-52425 Jülich, Germany.

D. Haaks, AERO-LASER GmbH., Unterfeldstrasse 12, D-82467 Garmisch-Partenkirchen, Germany.

(Received July 6, 1998; revised September 17, 1998; accepted September 21, 1998.)